



HAL
open science

Comparisons of models of electric drives for electric vehicles

Anatole Desreveaux, Mircea Ruba, Alain Bouscayrol, Gabriel Mihai Sirbu,
Claudia Martis

► **To cite this version:**

Anatole Desreveaux, Mircea Ruba, Alain Bouscayrol, Gabriel Mihai Sirbu, Claudia Martis. Comparisons of models of electric drives for electric vehicles. IEEE-VPPC'19, Oct 2019, Hanoi, Vietnam. hal-02925436

HAL Id: hal-02925436

<https://hal.science/hal-02925436>

Submitted on 29 Aug 2020

HAL is a multi-disciplinary open access archive for the deposit and dissemination of scientific research documents, whether they are published or not. The documents may come from teaching and research institutions in France or abroad, or from public or private research centers.

L'archive ouverte pluridisciplinaire **HAL**, est destinée au dépôt et à la diffusion de documents scientifiques de niveau recherche, publiés ou non, émanant des établissements d'enseignement et de recherche français ou étrangers, des laboratoires publics ou privés.

Comparisons of models of electric drives for electric vehicles

Anatole DESREVEAUX^{1*}, Mircea RUBA^{2*}, Alain BOUSCAYROL^{1*}, Gabriel Mihai SIRBU^{3*}, Claudia MARTIS^{2*}

¹ Univ. Lille, Arts et Metiers Paris Tech, Centrale Lille, HEI, EA 2697- L2EP, F-59000 Lille, France

² University of Technology of Cluj Napoca, Cluj-Napoca 400114, Romania

³ Renault Technologie Roumanie SRL, Bucarest, Romania

* PANDA, Grant Agreement 824256, <https://project-panda.eu/>

Abstract — The reduction of greenhouse gas emission is necessary to limit the global warming. Electrification of the transport sector is one solution. To accelerate the change, accurate and fast simulation program are one of the key issues. The choice of the accurate model is an important aspect to the simulation program. In this paper, different models of an electric drive for an electric vehicle are compared in terms of computation time and energy consumption. A static model will lead to divide the computation time by 100, by losing only 2% of accuracy

Keywords — Electric Vehicle, electric drive, modeling, Energetic Macroscopic Representation

I. INTRODUCTION

Reduction of greenhouse gas emissions and air pollution are major challenges for the transport sector. One solution is to use more and more electrified vehicles. According to the International Energy Agency, more than 100 million electrified vehicles in 2030 are required to limit the global warming to 2°C [1]. To fulfill this challenge, the automobile industry needs to speed up new vehicle developments. One of the key issues is to use the appropriate simulation programs.

Different models of the same system have to be used in function of the objective of the study [2] [3]. In electric drives (e-drives), dynamic models are required for the design of the system control [4]. But static models are often sufficient for the drive design, performance analysis or the energy management of a global system (e.g. electric vehicle or wind turbine) [5] [6]. Moreover, quasi-static models are also used for system analysis [7].

The objective of this paper is to compare dynamic and static models of an electric drive for simulation of an electric vehicle traction system. The Renault Zoe is considered as an example. The simulation results will be compared in terms of accuracy of the energy consumption and the computation time.

This paper is based on [8] with the following extensions:

- the regenerative braking is limited to 50%,
- the AC machine is a PMSM (instead of an IM)
- the computation time will be compared,
- real driving cycles will be considered instead of NEDC.

EMR (Energetic Macroscopic Representation) formalism [9] will be used to organize the different models in a unified way.

Section II presents the studied vehicle. In Section III, different models for the e-drive are presented. The different models are compared using urban and extra-urban driving cycles in Section IV.

II. STUDIED VEHICLE

A. Traction system of the studied vehicle

The studied vehicle is the commercial electric vehicle Renault Zoe (Fig. 1) [10]. This vehicle is composed of a battery, an electric drive connected to the mechanical transmission. The mechanical powertrain is a gearbox, a differential and two driven wheels (Fig. 2). Different parameters of the vehicle are given in Table 1.



Fig. 1: The Renault Zoe [10]

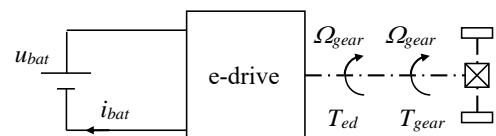


Fig. 2: Traction system of the studied EV

Table 1: Parameters of the studied vehicle

Weight	1468 kg
Battery	Li-ion NMC-22 kWh

B. Models of subsystems

The different subsystems are modeled considering classical assumptions in the objective of the design of the control scheme of the system.

A classical model of the battery is considered using a series resistance R_{bat} and an Open-Circuit Voltage (OCV) u_0 for a constant temperature (the OCV depends on the battery State of Charge (SoC) related to the current):

$$u_{bat} = u_0(\text{SoC}) - R_{bat}i_{bat} \quad (1)$$

The battery is connected to the electric drive. This electric drive gives the torque to the mechanical transmission. It will be described by different models in section III.

The gearbox links the torques, T_{ed} and T_{gear} , but also the rotation speeds, Ω_{wh} and Ω_{gear} , thanks to the gearbox ratio k_{gear} (assumption of no losses):

$$\begin{cases} T_{gear} = k_{gear}T_{ed} \\ \Omega_{gear} = k_{gear}\Omega_{wh} \end{cases} \quad (2)$$

The wheel links the torque T_{gear} and the traction force F_{wh} , but also the rotation speed Ω_{wh} and the car velocity v_{ev} , thanks to the wheel radius R_{wh} :

$$\begin{cases} F_{wh} = 1/R_{wh} T_{gear} \\ \Omega_{wh} = 1/R_{wh} v_{ev} \end{cases} \quad (3)$$

The electric vehicle has two types of brakes: electric and mechanic brakes. The mechanic brake force is added to the wheel force:

$$F_{tot} = F_{wh} + F_{br} \quad (4)$$

The Newton second's law expresses the derivative of the velocity v_{ev} as a function of the traction and resistive forces, F_{wh} , and F_{res} , where M is the vehicle equivalent dynamical mass:

$$M \frac{d}{dt} v_{ev} = F_{tot} - F_{res} \quad (5)$$

The resistive force is composed of a rolling force, a drag force and the slope.

$$F_{res} = F_{roll} + F_{aero} + F_{slope} \quad (6)$$

C. EMR and control of the traction system

EMR is based on two main principles. The causality principle imposes an integral relationship between output and inputs (i.e. outputs can only be delayed from inputs). The interaction principle indicates that the product of the action and reaction between two elements leads to the power exchanged by these elements.

Using inversion rules, the control scheme (blue pictograms) is systematically deduced from the EMR. Energy conversion elements (orange square or circles) are directly inverted while accumulation elements (crossed orange rectangle) are inverted using close-loop control loops (Fig.3). During the braking phase, the strategy distributes the braking energy between the mechanic brakes and the electric machine. The electric braking is limited to 50% of the total braking force.

From the EMR, a control scheme can be systematically deduced (blue pictogram). This control leads to define the reference of the e-drive torque T_{ed-ref} .

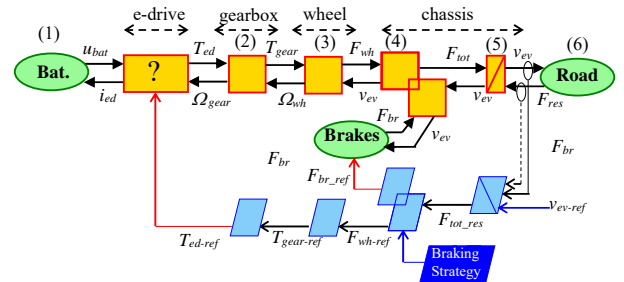


Fig. 3: EMR of the global vehicle

III. DIFFERENT MODELS OF THE E-DRIVE

A. Studied electric drive

The studied e-drive is composed of a 65 kW Permanent Magnet Synchronous Machine (PMSM) with its inverter (Fig. 4).

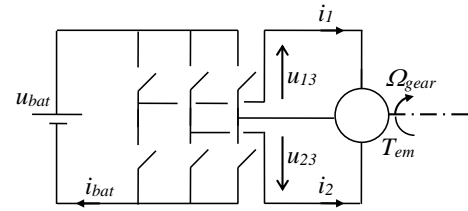


Fig. 4: Studied electric drive

B. Static model of the e-drive

A static model is first considered:

$$\begin{cases} T_{ed} = T_{ed-ref} \\ i_{vsi} = \frac{T_{ed}\Omega_{gear}}{u_{bat}\eta^k} \end{cases} \text{ with } k = \begin{cases} 1 & \text{if } T_{ed}\Omega_{gear} \geq 0 \\ -1 & \text{if } T_{ed}\Omega_{gear} < 0 \end{cases} \quad (7)$$

On the one hand, the efficiency η can be considered as a constant of 90%. On the other hand, an efficiency map can be used (Fig. 5). In EMR, the electric drive is considered as a multi-domain conversion element, i.e. orange circle (Fig. 6).

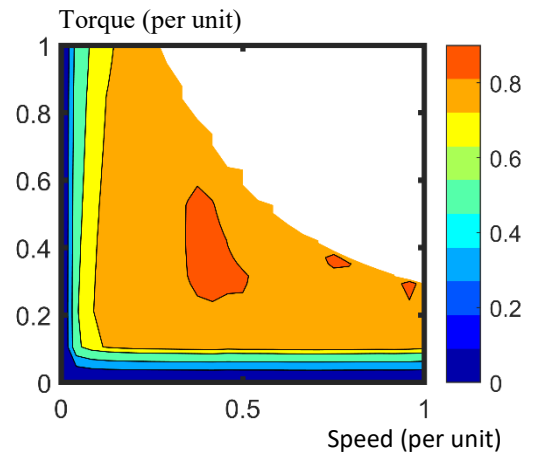


Fig. 5: Efficiency map of the electric drive of the Renault Zoe

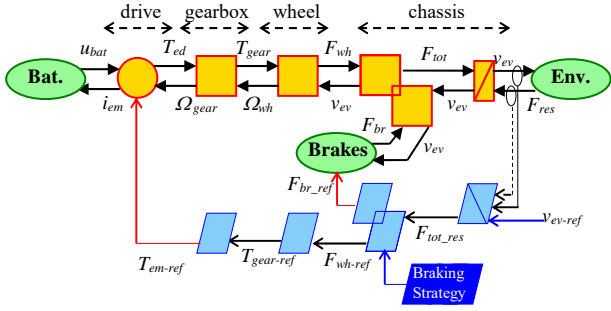


Fig. 6: EMR of the global vehicle with the static model for the e-drive

C. Dynamical model of the e-drive

The VSI is modeled on average values. A modulation vector $\underline{m}_{vsi} = [m_1, m_2]^t$ links the battery and modulated voltages, u_{bat} and $\underline{u}_{vsi} = [u_{13}, u_{23}]^t$, but also the machine and VSI currents $\underline{i}_{im} = [i_1, i_2]^t$ and i_{vsi} :

$$\begin{cases} u_{vsi} = m_{vsi} u_{bat} \\ i_{vsi} = m_{vsi}^t i_{em} \end{cases} \quad (8)$$

The machine is modeled in the classical (d,q) reference frame using the Park's transformation $[T(\theta_{d/s})]$. The actual stator voltages and currents, \underline{u}_{vsi} and \underline{i}_{im} , are expressed by the (d,q) voltages and currents, \underline{u}_{sdq} and \underline{i}_{sdq} :

$$\begin{cases} u_{sdq} = [T(\theta_{d/s})] u_{vsi} \\ i_{em} = [T(\theta_{d/s})]^{-1} i_{sdq} \end{cases} \quad (9)$$

Where $\theta_{d/s}$ is the position of the rotor flux. In this frame, equivalent stator windings can be defined in order to produce the same flux as the actual windings:

$$L_s \frac{d}{dt} i_{sdq} = \underline{u}_{sdq} - e_{sdq} - R_s i_{sdq} \quad (10)$$

Where L_s and R_s are the cyclic inductance and resistance of the stator winding. The electromechanical conversion leads to the torque T_{em} and the e.m.f. e_{sdq} from the currents and the rotation speed Ω_{gear} :

$$\begin{cases} T_{em} = k_1 \varphi_{rd} i_{sq} \\ e_{sdq} = f(i_{sdq}, \theta_{d/s}, \varphi_{rd}) \end{cases} \quad (11)$$

The different parts and the control are organized by EMR, (Fig. 9). The electromechanical conversion (11) is inverted, i_{sq} is given by the torque of the machine, i_{sd} depends of the flux weakening of the machine and it is given by the strategy.

$$\begin{cases} i_{sq.ref} = \frac{T_{em}}{k_1 \varphi_{rd}} \\ i_{sd.ref} = \end{cases} \quad (12)$$

The stator winding are inversed indirectly using controllers to invert the causal relation in (10).

$$u_{sdq.ref} = \underline{C}_{sdq}(t)(i_{sdq.ref} - i_{sdq.mes}) + e_{sdq} \quad (13)$$

The modulated voltages are calculated with the inversion of (9).

$$u_{vsi.ref} = [T(\theta_{d/s})]^{-1} u_{sdq} \quad (14)$$

The modulation vector is obtained by inversion of (8).

$$m_{vsi.ref} = \frac{u_{vsi.ref}}{u_{bat.mes}} \quad (15)$$

IV. COMPARISON OF THE E-DRIVE MODELS

Two real driving cycles, one urban and one extra-urban, are used to compare the different e-drive models. All the models are implemented in Matlab/Simulink © using the EMR library [11].

A. Urban real driving cycles

The urban trip is from the university campus "Cit  Scientifique" and Lille downtown (Fig. 7) and return in the same way. The trip is 14 km long for 40 min of driving (Fig. 8).



Fig. 7: real urban driving cycle

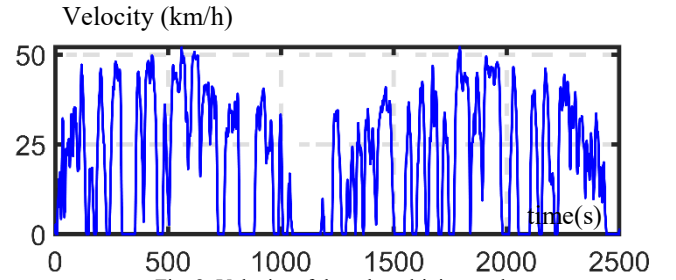


Fig. 8: Velocity of the urban driving cycle

The energy consumption of the different models is plotted in Fig. 10 and in results I Table 2.

The static model with constant efficiency has a computation time of 1.46 s and an energy consumption of 1.90 kWh. The efficiency map leads to a computation time of 2.16 s and an energy consumption of 1.94 kWh. The dynamical model has a computation time of 4 min and an energy consumption of 1.98 kWh. This last model is considered as a reference as it is the most accurate. The static models lead to divide the computation by 100 with an error of 2% to 4% in terms of energy consumption. The error (Fig. 11) is stabilized around 2 and 4 % respectively for the efficiency map and the constant efficiency.

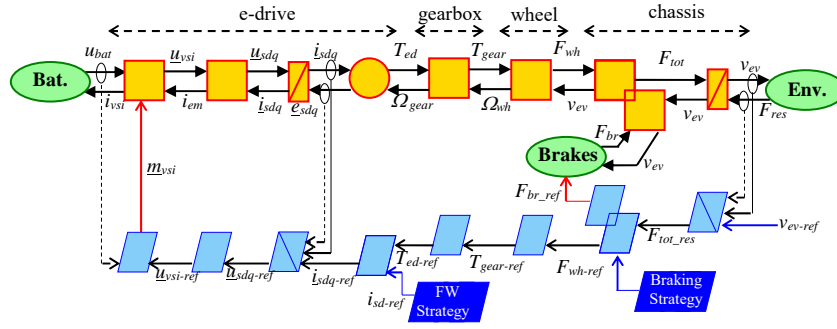


Fig. 9: EMR of the studied vehicle with the dynamic model of the e-drive

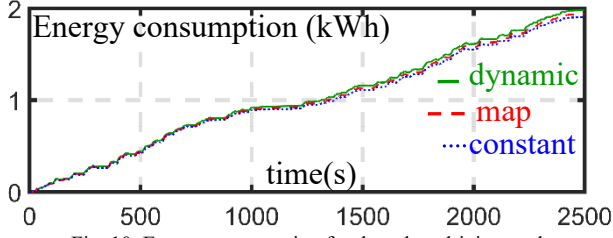


Fig. 10: Energy consumption for the urban driving cycle

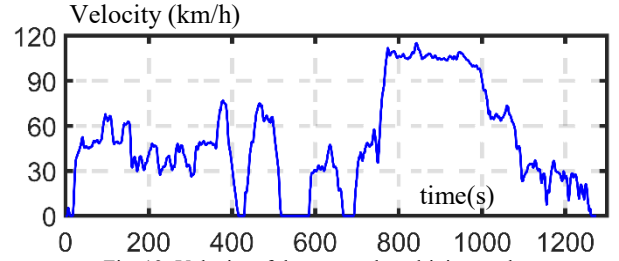


Fig. 13: Velocity of the extra urban driving cycle

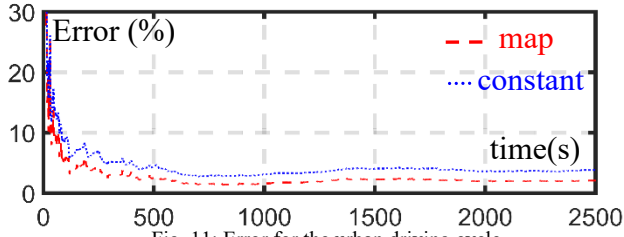


Fig. 11: Error for the urban driving cycle

The energy consumption is calculated for each model (Fig. 14). The different results can be found in the

Table 3. The static model with a constant efficiency has a computation time of 0.87 s and an energy consumption of 2.88 kWh. The model with the efficiency map is computed in 1.47s for an energy consumption of 2.80 kWh. The dynamical model is computed in 3 min and 15 s for an energy consumption of 2.88 kWh.

Once again the static models lead to divide the computation time by 100 with an error only between 1.5% to 3%. The error (Fig. 15) is stabilized around 1.5 and 3 % for the efficiency map and the constant efficiency

Table 2: Comparison for an urban driving cycle

Model of the e-drive	Static model Constant efficiency	Static model Efficiency map	Dynamic model
Computation time	1.76 s	2.16 s	244.66 s
Energy consumption	1.90 kWh (error 4%)	1.94 kWh (error 2%)	1.98 kWh (ref)

B. Real extra urban driving cycles

The extra urban trip is from the university campus and city of Baisieux (Fig. 12). The return is made using a highway. The trip is 17.54 km long with a duration of 12 min. The trip is composed of different sections between 30 km/h and 110 km/h (Fig. 13).



Fig. 12: real extra urban driving cycle

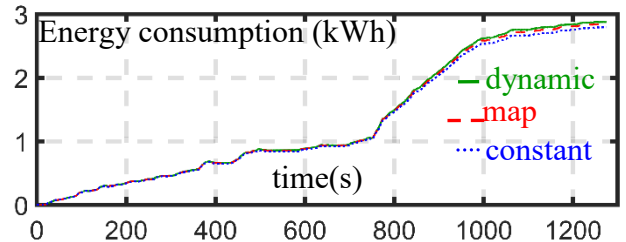


Fig. 14: Energy consumption for the extra-urban driving cycle

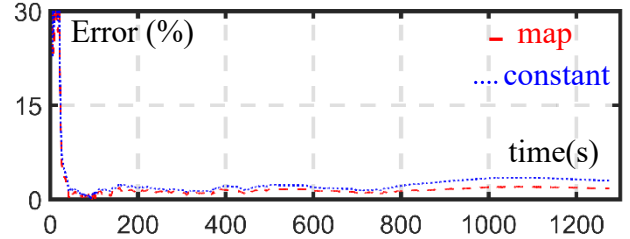


Fig. 15: Error for the extra-urban driving cycle

Table 3: Comparison for an extra urban driving cycle

Model of the e-drive	Static model Constant efficiency	Static model Efficiency map	Dynamic model
Computation time	1.16 s	1.47 s	137.38 s
Energy consumption	2.79 kWh (error 3.1%)	2.84 kWh (error 1.4%)	2.88 kWh (reference)

V. CONCLUSION

For the studied vehicles and driving cycles, two static models are proposed. Globally, they have the computation time but the efficiency map have the error divided by 2 in comparison to the constant efficiency. In comparison with the dynamic model the computation time is divided by 100 and across 2%. In function of the studied objective, different models of electric drives can be selected.

ACKNOWLEDGMENT

The research leading to these results has received funding from the European Community’s Horizon 2020 Program under grant agreement No. 824256 (PANDA).

REFERENCES

[1] “Global EV outlook 2018, towards cross-modal electrification”, International Energy Agency report, 2018

[2] D. W. Gao, C. Mi, and A. Emadi, “Modeling and simulation of electric and hybrid vehicles”, *Proceeding of the. IEEE*, vol. 95, no. 4, pp. 729–745, April 2007.

[3] C. C. Chan, A. Bouscayrol, K. Chen, “Electric, Hybrid and Fuel Cell Vehicles: Architectures and Modeling”, *IEEE trans. on Vehicular Technology*, vol. 59, no. 2, pp. 589-598, Feb. 2010.

[4] Seung-Ki Sul, “Control of electric machine drive systems”, ISBN: 978-0-470-59079-9, Wiley-IEEE Press, February 2011.

[5] T. Sun, B.K. Kim, J.H. Lee, J.P Hong, “Determination of parameters of motor simulation module employed in ADVISOR”, *IEEE trans. On Magnetics*, vol. 44, no. 6, June 2008.

[6] J. O. Estima and A. J. Marques Cardoso, “Efficiency Analysis of Drive Train Topologies Applied to Electric/Hybrid Vehicles”, *IEEE transactions on Vehicular Technology.*, vol. 61, no. 3, pp. 1021-1031, Feb. 2012.

[7] L. Guzzella, A. Sciarretta, “Vehicle Propulsion Systems, introduction to modelling and optimization”, Springer, ISBN-13: 978-3642438479, 3rd edition, January 2015.

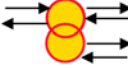
[8] T. Letrouvé, A. Bouscayrol, W. Lhomme, N. Dollinger, F. Mercier Calvairac, “ Different models of a traction drive for an electric vehicle simulation", *IEEE-VPPC'10*, Lille (France), September 2010.

[9] A. Bouscayrol, J. P. Hautier, B. Lemaire-Semail, "Graphic Formalisms for the Control of Multi-Physical Energetic Systems", *Systemic Design Methodologies for Electrical Energy, tome 1, Analysis, Synthesis and Management, Chapter 3*, ISTE Willey editions, October 2012, ISBN: 9781848213883.

[10] Renault Zoe [Online] Available: <http://www.renault.fr/vehicules/vehicules-electriques/zoe>.

[11] EMR website [Online] Available: <https://www.emrwebsite.org/>.

Appendix A: EMR Pictograms

	Source element (energy source)		Accumulation element (energy storage)		Indirect inversion (closed-loop control)
	Mono-physical conversion element		Mono-physical coupling element (energy distribution)		Direct inversion (open-loop control)
	Multi-physical conversion element		Multi-physical coupling element (energy distribution)		Coupling inversion (energy criteria)